

## Double scattering and infrared sensitivity for nuclear targets

Keith Kastella

*Institute for Theoretical Physics, State University of New York at Stony Brook, Stony Brook, New York 11794-3840*

(Received 29 May 1987)

Single-particle and two-particle inclusive cross sections for  $p + A \rightarrow \text{hadrons}$  at high  $P_{\perp}$  are studied using QCD in a multiple-scattering expansion. Single-particle cross sections are shown to be infrared divergent. In contrast with this, the leading contribution to nonplanar two-particle inclusive scattering is calculated without a cutoff. The result is consistent with the available data, but a large bremsstrahlung background masks the multiple-scattering signal. This background can be eliminated by studying the forward/backward asymmetry of the events in the projectile-nucleon c.m. system. This asymmetry is  $\sim 0.1$  on a W target at 800-GeV laboratory energy and is sensitive to the small- $x$  structure of the target.

### I. INTRODUCTION

The  $A$  dependence of high- $P_{\perp}$  single-hadron production on nuclear targets has been measured and found to vary as  $A^{\alpha}$  with  $\alpha \sim 1.1-1.3$  (Ref. 1). Double-hadron production has also been studied with similar results.<sup>2</sup> Aside from its intrinsic interest, the European Muon Collaboration (EMC) effect and speculation on quark-gluon-plasma formation mechanisms have stimulated further study of this problem. A number of authors have suggested that this  $A$  dependence is an  $O(\alpha_s^4)$  effect caused by double scattering within the target.<sup>3</sup> This idea has been pursued quantitatively, and fits to data have been produced using QCD in a multiple-scattering expansion for single hadrons<sup>4</sup> and for planar hadron pairs.<sup>5</sup> In order to eliminate soft scattering, an arbitrary infrared cutoff, which we will denote by  $t_{\min}$ , must be used in this double-scattering model. In this paper we examine the role of soft scattering on single-particle and two-particle inclusive cross sections. We also give predictions for nonplanar cross sections, which can be calculated without any cutoff. Finally, we propose and calculate a new quantity, the forward-backward asymmetry for nonplanar scattering, which eliminates the bremsstrahlung background encountered in nonplanar events.

The problem for single-particle cross sections is similar to the problem encountered in defining a total cross section for Thomson scattering in elementary mechanics. In Thomson scattering the differential cross section is proportional to  $t^{-2}$ . Its integral is divergent at the lower limit. If it is cut off at some value  $t = t_{\min}$ , the resulting total cross section is dominated by soft scattering and scales as  $t_{\min}^{-1}$ .

We shall see that in double-scattering divergences at  $O(\alpha_s^4)$  are caused by kinematic configurations that mimic  $O(\alpha_s^2)$  single-scattering events. These events involve one hard collision and one soft collision so that they are proportional to the total cross section for single scattering. This suggests that the leading divergences in the model might also go as  $t_{\min}^{-1}$ . However, a more de-

tailed analysis shows that these leading divergences cancel, while  $\ln(t_{\min})$  terms remain.

In addition, we shall investigate the leading contribution of multiple scattering to nonplanar two-particle inclusive events. This turns out to be calculable without a cutoff, since these events cannot be mimicked by lowest-order single scattering. Unfortunately, there is a large  $O(\alpha_s^3)$  background from bremsstrahlung which masks the multiple-scattering signal. This problem is avoided by calculating the forward-backward asymmetry of the nonplanar two-particle inclusive cross section. This is also calculable in a cutoff-free manner, and cleanly separates double-scattering events from the background. Surprisingly, the small-Feynman- $x$  structure of the target plays an important role in this asymmetry.

The paper is organized as follows. In Sec. II we review the application of multiple-scattering theory to the parton model and derive expressions for single-particle and two-particle inclusive cross sections, extending existing results slightly to include nonplanar two-particle events. In Sec. III we analyze the infrared behavior of the single-particle result for the standard multiple-scattering formalism<sup>4</sup> and show that it is infrared sensitive. In Sec. IV we discuss the scales relevant to nonplanar multiple scattering and bremsstrahlung. We then compare numerical results for nonplanar two-particle inclusive scattering with data. These points are calculated without any cutoff and are consistent with the data at large momentum transfers ( $P_{\perp} > 1$  GeV). No shadowing or absorption effects are included in this calculation. In Sec. V we present an analysis of the multiple-scattering-induced forward-backward asymmetry of the two-particle inclusive events. The bremsstrahlung background automatically cancels in this calculation. The small- $x$  sensitivity of this asymmetry is found to be rather strong and the gluon structure of the target plays the dominant role in both its magnitude and its sign. In Sec. VI we give a brief summary and speculate about possible directions for future work on this problem. In the Appendix we derive the parton-model result for hard-bremsstrahlung scattering.

## II. MULTIPLE-SCATTERING THEORY IN THE PARTON MODEL

In this section we review the multiple-scattering formalism as it has been applied to the parton model in the literature.<sup>3-5</sup> This sets the context and defines notation for the rest of the paper. The reader already familiar with multiple-scattering theory may wish to skip directly to Eq. (2.9) where we modify the result of Lev and Petersson,<sup>5</sup> describing planar two-particle inclusive scattering, in order to obtain an expression for nonplanar events. Unlike the planar scattering considered in Ref. 5, this new expression can be calculated without a cutoff.

We now proceed with the calculation of single-particle and two-particle inclusive cross sections for double scattering on nuclear targets. Since we are primarily concerned with qualitative features of the model, we shall ignore momentum-transfer scaling and transverse-momentum smearing in the structure functions  $F_h^i(x)$  and fragmentation functions  $D_i^h(z)$  for hadrons  $h$  and partons  $i$ . First, consider the single-particle cross section for an incoming parton  $i$  with momentum  $p$  to produce a parton  $j$  with momentum  $p'$  after arbitrarily many scatterings. This is expressed in terms of the sum over all fixed numbers of scatterings as

$$H^{ij}(p \rightarrow p') = \sum_{n=1}^{\infty} H_n^{ij}(p \rightarrow p'). \quad (2.1)$$

Here  $H_n^{ij}$  is the contribution to  $H^{ij}$  made by  $n$  scatterings. In the parton model this is an incoherent sum. This makes sense only if the momentum transfer at each

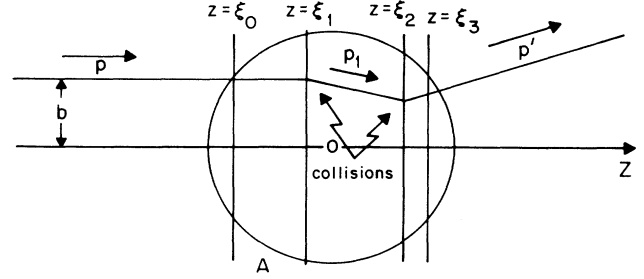


FIG. 1. Picture in the rest frame of the target of a double-scattering event. Collisions occur in the planes  $z = \xi_1$  and  $z = \xi_2$ .

collision is much greater than  $\lambda^{-1}$  where  $\lambda$  is the mean free path. When the momentum transfer becomes small, the coherent effects, which we ignore here, can become important.

How do we calculate the  $H_n^{ij}$ ? The double collision process is pictured in Fig. 1. The parton makes the transition from momentum state  $p$  to momentum state  $p'$  through a sequence of  $n - 1$  intermediate states  $p_i$ . The final parton state is  $p_n = p'$ . These transitions occur in planes  $z = \xi_i$ . From each intermediate state  $p_i$  the parton can do one of two things: it can scatter into the next state  $p_{i+1}$  in the sequence or it can scatter into some other state. In the multiple-scattering model, this second process is represented by an exponential absorption term  $G^{ij}$ . The nucleus is taken to be a sphere of radius  $R = R_0 A^{1/3}$  with constant number density  $\rho = 3/4\pi R_0^3$ . We write

$$H_n^{ij}(p \rightarrow p') = \rho^n \sum_{k, \dots, l} \int \frac{d^3 p_1}{E_1} \dots \frac{d^3 p_{n-1}}{E_{n-1}} h^{ik}(p \rightarrow p_1) \dots h^{lj}(p_{n-1} \rightarrow p_n) G^{ij}(p, p_1, \dots, p_n), \quad (2.2)$$

where  $h^{ik}(p \rightarrow q)$  is the conventional parton-model expression for the one-particle inclusive cross section of a parton on a single-nucleon target.<sup>6</sup>

$$h^{ij}(p \rightarrow p') = \frac{1}{\pi} \sum_m \int dx F_N^m(x) \frac{d\sigma^{ij}}{d\hat{t}}(\hat{s}, \hat{u}, \hat{t}) \delta \left[ 1 + \frac{\hat{t} + \hat{u}}{\hat{s}} \right], \quad (2.3)$$

with  $m$  labeling the partons in a nucleus  $N$ . In order to simplify the expression for  $G^{ij}$  at high energies, we ignore deflections perpendicular to the beam direction. This gives

$$G^{ij}(p, p_1, \dots, p_n) = 2\pi \int b db \int_{\xi_0}^{\xi_{n+1}} d\xi_1 \dots \int_{\xi_{n-1}}^{\xi_{n+1}} d\xi_n \exp \left[ -\rho \sum_{k=0}^n \sigma_k(p_k)(\xi_{k+1} - \xi_k) \right]. \quad (2.4)$$

In this expression,  $b$  is the impact parameter with  $0 \leq b \leq R$  and  $-(R^2 - b^2)^{1/2} = \xi_0 \leq \xi_1 \leq \dots \leq \xi_n \leq \xi_{n+1} = (R^2 - b^2)^{1/2}$  (see Fig. 1). The total cross section for a parton of flavor  $k$  and momentum  $p_k$  is

$$\sigma_k(p_k) = \sum_m \int \frac{d^3 p'}{E'} h^{km}(p_k \rightarrow p'). \quad (2.5)$$

In this definition of  $\sigma_k(p_k)$  symmetry factors for identical particles are incorporated into  $h^{km}$ . Proper treatment of this factor is, of course, crucial for obtaining the cancellation of the leading  $t_{\min}$  terms.

Referring to Eq. (2.3), we note that for typical cross sections involving gluon exchange,  $d\sigma/dt \propto \alpha^2 t^{-2}$ , and Eq. (2.5) must be cut off at  $t=0$  with a mass-squared parameter  $t_{\min}$ . In Ref. 4, transverse-momentum smearing is included in the structure functions and it is suggested that the inclusion of this effect necessitates cutting off the integral. As we see in this example, even with no transverse-momentum smearing, the integral must be cut off in order to obtain a finite result.

In order to obtain an expression in terms of initial- and final-state hadrons one must fold in their structure and fragmentation functions. Defining the measure

$$d(F_h^i D_j^{h'}) \equiv dx F_h^i(x) \frac{dz}{z^2} D_j^{h'}(z),$$

this results in

$$E_{h'} \frac{d\sigma}{d^3P_{h'}} \Big|^{h+A \rightarrow h'+X} = \sum_{i,j} \int d(F_h^i D_j^{h'}) H^{ij}(p \rightarrow p'). \quad (2.6)$$

In this expression and in the following, capital letters are used for hadron momenta, while the parton momenta are written in lower-case letters.

To relate Eq. (2.6) to the hadron-nucleon cross section, we expand it in  $R$  and collect powers of  $R \sim A^{1/3}$ . This yields

$$E_{h'} \frac{d\sigma}{d^3P_{h'}} \Big|^{h+A \rightarrow h'+X} = (A + c_2 A^{4/3} + \dots) E_{h'} \frac{d\sigma}{d^3P_{h'}} \Big|^{h+N \rightarrow h'+X}, \quad (2.7)$$

where

$$c_2 = \frac{9}{16\pi R_0^2} \sum_{ij} \int d(F_h^i D_j^{h'}) \left[ \sum_k \int \frac{d^3p_1}{E_1} h^{ik}(p \rightarrow p_1) h^{kj}(p_1 \rightarrow p') \right. \\ \left. - [\sigma_i(p) + \sigma_j(p')] h^{ij}(p \rightarrow p') \right] / \sum_{ij} \int d(F_h^i D_j^{h'}) h^{ij}(p \rightarrow p'). \quad (2.8)$$

In (2.8), the first term in large parentheses gives two scatterings into the measured final state, while the second term corresponds to one hard scattering and one absorptive collision.

By direct extension, this formalism can be used to describe two-particle inclusive scattering:<sup>5</sup>

$$E_3 E_4 \frac{d^6\sigma}{d^3P_3 d^3P_4} \Big|^{h+A \rightarrow h_3+h_4+X} = (A + d_2 A^{4/3} + \dots) E_3 E_4 \frac{d^6\sigma}{d^3P_3 d^3P_4} \Big|^{h+N \rightarrow h_3+h_4+X}. \quad (2.9)$$

There are two distinct situations described by this expression. The first is that in which the detected particles and the beam all lie in the same plane, as discussed in Ref. 5. In this case, both absorption and scattering terms analogous to those in Eq. (2.8) are present at  $O(\alpha_s^4)$ . The second situation, to be considered here in some detail, is that in which the beam and produced particles do not lie in a plane. For this type of scattering, no  $O(\alpha_s^2)$  processes contribute, so there can be no  $O(\alpha_s^4)$  absorption terms. The double-scattering contribution will always contain two hard collisions and we avoid the  $t=0$  region encountered in planar two-particle inclusive scattering and single-particle inclusive scattering. The two leading contributions to these nonplanar events are bremsstrahlung  $O(A\alpha_s^3)$  and double scattering  $O(A^{4/3}\alpha_s^4)$ .

The three nonabsorption processes that contribute to  $O(A^{4/3}\alpha_s^4)$  are pictured in Fig. 2. This time, the expansion in powers of  $A^{1/3}$  results in the leading correction to single scattering (analogous to  $c_2$  above)

$$d_2^{\text{nonplanar}} = \frac{9}{16\pi R_0^2} \sum_{ijk} \int d(F_h^i D_j^{h_3} D_k^{h_4}) \\ \times \left[ \int \frac{d^3p_1}{E_1} [g^{ik}(p \rightarrow p_1+p_4) h^{kj}(p_1 \rightarrow p_3) + g^{ik}(p \rightarrow p_1+p_3) h^{kj}(p_1 \rightarrow p_4) \right. \\ \left. + h^{ik}(p \rightarrow p_1) g^{kj}(p_1 \rightarrow p_3+p_4)] \right] \\ \times \left[ E_3 E_4 \frac{d^6\sigma}{dP_3^3 dP_4^3} \Big|^{h+N \rightarrow h_3+h_4+X} \right]^{-1}. \quad (2.10)$$

The terms of the numerator correspond in the order given to (a)–(c) of Fig. 2. The denominator in this expression,

$$E_3 E_4 \frac{d^6\sigma}{d^3P_3 d^3P_4} \Big|^{h+N \rightarrow h_3+h_4+X},$$

is the  $O(\alpha_s^3)$  inclusive  $2 \rightarrow 3$  double-differential bremsstrahlung cross section (see the Appendix). The  $g^{ij}$  are the  $O(\alpha_s^2)$  inclusive  $2 \rightarrow 2$  cross sections for the various subprocesses:<sup>5</sup>

$$\begin{aligned}
g^{ij}(p_i \rightarrow p_j p_{j'}) &\equiv E_j E_{j'} \frac{d^6 \sigma}{d^3 p_j d^3 p_{j'}} \Big|_{q_i + N \rightarrow q_j + q_{j'} + X} \\
&= \frac{1}{2\pi} \sum_m \int \frac{dx}{x} F_N^m(x) \frac{d\sigma^{ij}}{d\hat{t}}(\hat{s}, \hat{u}, \hat{t}) \delta^4(p_i + p_m - p_j - p_{j'}), \quad (2.11)
\end{aligned}$$

where all momenta are coplanar. Nonplanar scattering will be evaluated numerically and compared with data in Sec. IV.

### III. CUTOFF DEPENDENCE OF ONE-PARTICLE INCLUSIVE DOUBLE SCATTERING

Consider the contribution of double scattering to the single-hadron production cross section as depicted in Fig. 1. This multiple-scattering process is experimentally indistinguishable from a single-scattering event, and, in the multiple-scattering model, the Born approximation probabilities for the two processes are added incoherently to obtain the total probability. As either momentum transfer becomes small, the cross section equation (2.7) diverges. In the following we show that if this is regulated with an infrared cutoff, then the final result contains a nontrivial cutoff dependence.

If, instead of including absorption as in the multiple-scattering expansion equation (2.7), one models the double-scattering single-particle inclusive cross section naively as the product of two Born cross sections regulated by an infrared cutoff and integrated over intermediate states, the result diverges with a leading term

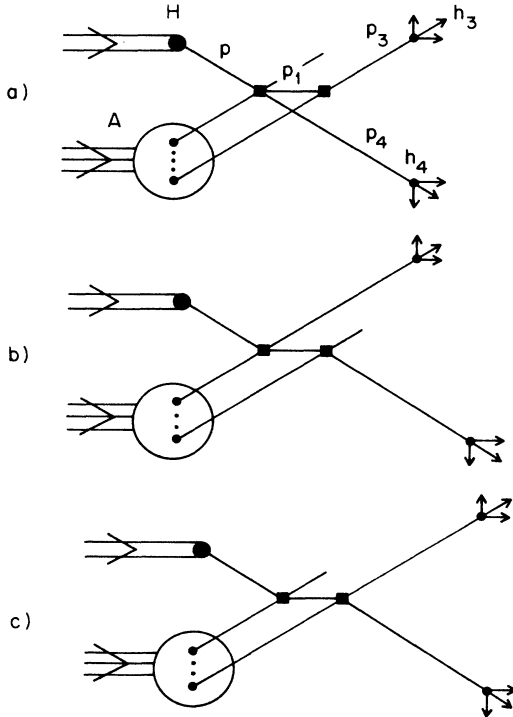


FIG. 2. Three possibilities for producing a hadron pair contributing to Eqs. (2.10) and (2.13).

that goes as  $t_{\min}^{-1}$ . We now show that in (2.7), this term is also present, but is canceled by the absorption terms, while subleading  $\ln t_{\min}$  terms remain. This logarithmic cutoff dependence is consistent with the cutoff insensitivity reported in Ref. 4. The cancellation of the leading singularity can be understood as a consequence of destructive interference between the soft two-gluon-exchange graphs and the scattering graph.

The infrared-divergent parts of the double-scattering term are contained in the expression for  $c_2$ , Eq. (2.8). Dropping the structure functions (which play no role in this discussion) and ignoring constant factors, this is

$$\begin{aligned}
c_2^{\text{div}} &\sim \int \frac{d^3 p_1}{E_1} \frac{d\sigma}{dt_1}(p \rightarrow p_1) \delta \left[ 1 + \frac{\hat{t}_1 + \hat{u}_1}{\hat{s}_1} \right] \\
&\quad \times \frac{d\sigma}{dt_2}(p_1 \rightarrow p') \delta \left[ 1 + \frac{\hat{t}_2 + \hat{u}_2}{\hat{s}_2} \right] \\
&\quad - [\sigma(p) + \sigma(p')] \frac{d\sigma}{dt}(p \rightarrow p') \delta \left[ 1 + \frac{\hat{t} + \hat{u}}{\hat{s}} \right]. \quad (3.1)
\end{aligned}$$

The first term is the product of Born cross sections, while the negative terms describe absorption. The intermediate state,  $p_1$ , is on shell and massless. Here we examine the  $\hat{t}_1 \sim 0$  ( $\theta_1 \sim 0$ ) region. In this region we may write

$$\frac{\hat{t}_2 + \hat{u}_2}{\hat{s}_2} = \frac{\hat{t} + \hat{u}}{\hat{s}} + O\left(\frac{\hat{t}_1}{\hat{s}_1}\right), \quad (3.2)$$

so the first term of (3.1) becomes

$$\begin{aligned}
&\int \frac{d^3 p_1}{E_1} \frac{d\sigma}{dt_1}(p \rightarrow p_1) \delta \left[ 1 + \frac{\hat{t}_1 + \hat{u}_1}{\hat{s}_1} \right] \frac{d\sigma}{dt_2}(p_1 \rightarrow p') \\
&\quad \times \delta \left[ 1 + \frac{\hat{t}_2 + \hat{u}_2}{\hat{s}_2} \right] \sim \sigma(p) \frac{d\sigma}{dt}(p \rightarrow p') \delta \left[ 1 + \frac{\hat{t} + \hat{u}}{\hat{s}} \right]. \quad (3.3)
\end{aligned}$$

This term then cancels identically with the  $\sigma(p)$  absorption term while the  $O(\hat{t}_1/\hat{s}_1)$  corrections can generate subleading divergences. The analysis of (3.1) in the  $\hat{t}_2 \sim 0$  region is identical and the leading divergent contribution of the integral cancels with the  $\sigma(p')$  absorption term.

It might seem surprising that this essentially classical sequential-scattering picture should result in the cancellation of the leading  $t_{\min}^{-1}$  divergence. How can we understand this in terms of quantum mechanics? First, consider a single scattering of momentum transfer  $t$ . The probability for this process is proportional to the diagrams of Fig. 3. The first diagram contributes to scattering at all momentum transfers, while the second

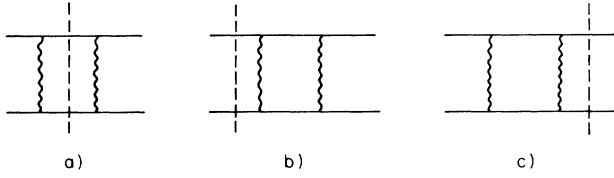


FIG. 3. Single-scattering diagrams contributing to double scattering. Hard-scattering contribution (a) and soft scattering (b) and (c) all give contributions of order  $\alpha_s^2$ .

two diagrams only contribute to the forward-scattering region. By the unitarity of the  $S$  matrix, the sum of these three diagrams, integrated over all final states, vanishes, and the second two diagrams are proportional to the total cross section  $\sigma_{\text{tot}}$ . Using this complete set of diagrams at  $O(\alpha_s^2)$ , we can express the total differential cross section  $d\bar{\sigma}/dt$ , including the forward-scattering region, as

$$\frac{d\bar{\sigma}}{dt} = \frac{d\sigma}{dt} - \sigma_{\text{tot}}\delta(t), \quad (3.4)$$

where  $d\sigma/dt$  is the usual differential cross section of Fig. 3(a).

We may now use this to express the cross section for two-particle inclusive double scattering as the product of two single scatterings, including this forward-scattering term. This gives

$$\frac{d\sigma^{\text{double}}}{dt_1 dt_2} \propto \frac{1}{R_0^2} \frac{d\bar{\sigma}}{dt_1} \frac{d\bar{\sigma}}{dt_2}. \quad (3.5)$$

To illustrate how this works we use this expression in a one-dimensional toy model using  $d\sigma/dt \equiv \alpha_s^2/t^2$ . Cutting off the  $t$  integral for the total cross section at  $t=t_{\text{min}}$ , this definition gives  $\sigma_{\text{tot}} = \alpha_s^2/t_{\text{min}} + \text{finite}$ . For double scattering with a total momentum transfer  $T=t_1+t_2$  we have

$$\begin{aligned} \frac{d\sigma^{\text{double}}}{dT} &= \int_{t_{\text{min}}}^{T-t_{\text{min}}} dt_1 \frac{d\sigma^{\text{double}}}{dt_1 dt_2} \\ &\propto \frac{1}{R_0^2} \left[ \int_{t_{\text{min}}}^{T-t_{\text{min}}} dt_1 \frac{\alpha_s^2}{t_1^2} \frac{\alpha_s^2}{(T-t_1)^2} - 2\sigma_{\text{tot}} \frac{d\sigma}{dT} \right]. \end{aligned} \quad (3.6)$$

As can be seen by inspection, the leading  $t_{\text{min}}$ -divergent terms of the integral are proportional to  $t_{\text{min}}^{-1}$  and cancel with the  $t_{\text{min}}$  dependence of  $\sigma_{\text{tot}}$ . Observe that  $\ln(t_{\text{min}}/T)$  terms remain uncanceled.

In a similar way we can calculate the subleading terms of Eq. (3.1). In the  $t_1 \sim 0$  region, these are generated by terms with higher powers of  $\theta_1$  in the integrand and are most easily obtained by cutting off the  $\theta_1$  integral at  $\theta_{\text{min}} = (t_{\text{min}}/s_1)^{1/2}$ . The form of the divergence can be derived by examining a particular case. In order to obtain typical behavior, we use the cross section for the scattering of unlike quarks:<sup>7</sup>

$$\frac{d\sigma^{q_a q_b \rightarrow q_a q_b}}{dt} = \frac{4\pi\alpha^2}{9s^2} \frac{s^2 + u^2}{t^2} = \frac{8\pi\alpha^2}{9} \left[ \frac{1}{t^2} + \frac{1}{st} + \frac{1}{2s^2} \right]. \quad (3.7)$$

The  $1/s^2$  term makes no contribution to the divergence since  $s$  is nonvanishing. The  $1/st$  term generates logarithmic divergences at the leading order, so these are canceled by the absorption term as in (3.3). Only the  $1/t^2$  term generates a noncanceling divergence.

For simplicity, consider right-angle scattering of a projectile parton at energy  $E$  scattering into a state with energy  $E' < E$ . The target partons have initial energies  $x_1 E$  and  $x_2 E$ . The kinematics of two collisions are described by

$$\begin{aligned} \hat{s}_1 &= 4x_1 E^2, \quad \hat{t}_1 = -2E_1 E(1 - \cos\theta_1), \\ \hat{u}_1 &= -2x_1 E_1 E(1 + \cos\theta_1), \\ \hat{s}_2 &= 2x_2 E E_1(1 + \cos\theta_1), \\ \hat{t}_2 &= -2E_1 E'(1 - \sin\theta_1 \cos\phi_1), \quad \hat{u}_2 = -2x_2 E E'. \end{aligned} \quad (3.8)$$

The first subleading corrections to the integrand are proportional to  $\theta_1 \cos\phi_1$ , and so vanish when  $\phi_1$  is integrated from 0 to  $2\pi$ . The second subleading term is nonvanishing and equal to

$$\begin{aligned} -4\pi \ln(\theta_{\text{min}}) \frac{8\pi\alpha^2 \bar{x}_2^2}{9EE'} \frac{d\sigma}{d\hat{t}} \left[ \frac{1}{4} + \frac{1}{2x_1} \left[ \bar{x}_2 + 1 \right] \right. \\ \left. - \frac{\bar{x}_2}{4} \left[ 1 - \frac{\bar{x}_2}{x_1} \right] \frac{\partial}{\partial x_2} + \frac{\bar{x}_2^2}{4} \frac{\partial^2}{\partial x_2^2} \right] \delta(x_2 - \bar{x}_2) \end{aligned} \quad (3.9)$$

with

$$\bar{x}_2 \equiv \frac{E'}{2E - E'}.$$

In (3.6) the derivatives act on all remaining  $x_2$ 's outside of the  $\delta$  function.

In the  $t_2 \sim 0$  region the behavior is similar. This region is given by  $\theta_1 \sim \pi/2$  and  $\phi_1 \sim 0$ . Again, the first subleading terms vanish because of the symmetry of the region of integration. The logarithmic divergences do not vanish and are given by

$$\begin{aligned} -2\pi \ln(\theta_{\text{min}}) \frac{8\pi\alpha^2 \bar{x}_1^2 E}{9E'^3} \frac{d\sigma}{d\hat{t}} \left[ \frac{3}{2} - \frac{2\bar{x}_1 E'}{x_2 E} \right. \\ \left. - \left[ 3 - \frac{(1 + \bar{x}_1)E'}{x_2 E} \right] \bar{x}_1 \frac{\partial}{\partial x_1} + 2\bar{x}_1^2 \frac{\partial^2}{\partial x_1^2} \right] \delta(x_1 - \bar{x}_1) \end{aligned} \quad (3.10)$$

with

$$\bar{x}_1 \equiv \frac{E'}{2E - E'}.$$

The energy dependence of the divergences in the  $t_1 \sim 0$  and  $t_2 \sim 0$  regions is quite different, since the first case corresponds to a correction to absorption from a state with energy  $E$ , while the second case corresponds to a correction to absorption from a state with energy  $E'$ . Because of this, the two divergences cannot cancel.

The vanishing of the first subleading terms here is not peculiar to right-angle scattering. For  $t_1 \sim 0$  scattering into a final state at angle  $\theta'$ , the  $O(\theta_1)$  correction to the integrand comes from

$$\hat{t}_2 = -2E_1 E [1 - \sin\theta_1 \cos\phi_1 \sin\theta' + O(\theta_1^2)],$$

so terms in the integrand proportional to  $\theta_1^{-2}$  are linear in  $\cos\phi_1$  and vanish under the  $\phi_1$  integral for any value of  $\theta'$ .

Despite the remarkable cancellation of the leading divergences in the double-scattering expansion, there are subleading terms that exhibit a logarithmic cutoff dependence. We now turn to the question of finding a measurable quantity that is calculable without a cutoff.

#### IV. NONPLANAR SCATTERING

We have seen that the cutoff dependence of double scattering derives from the soft-scattering part of the integral over intermediate states. This problem can be avoided if we eliminate this part of the kinematic domain. In a double-scattering process with one soft collision, the measured particle and the debris must always lie in the same plane, as they do in single-scattering events (ignoring the transverse-momentum distribution of the target and projectile). To carry out an experiment involving only hard collisions, we must measure two produced particles. Then for this model, those double-scattering events, in which the projectile and the two outgoing particles are not coplanar will contain only hard collisions. There are already some data on events of this type.<sup>8,9</sup>

To examine this idea in detail, consider the semi-inclusive double-differential cross section for proton-induced production of two hadrons on a nuclear target  $A$ . This is defined in Eqs. (2.12) and (2.13). Following the conventions in Refs. 8 and 9, we analyze the problem in the proton-nucleon center-of-mass system (c.m.s.) (not the proton-nucleus c.m.s.) (Fig. 4). Let  $P_3$  and  $P_4$  be the energies of the produced hadrons with  $P_3 > P_4$  (we assume  $P_3 \gg m_3$  and  $P_4 \gg m_4$ , and so ignore masses in the kinematics). Define  $m' = P_{3\perp} + P_{4\perp}$ . Let  $\theta_i$  be the angle between  $\mathbf{P}_i$  and the beam, while  $\phi_4$  is the angle between the  $\mathbf{P}_4$ -beam plane and the  $\mathbf{P}_3$ -beam plane. We define  $p_{\text{out}}$  as the component of  $\mathbf{P}_4$  perpendicular to the  $\mathbf{P}_3$ -beam plane. This is given by  $p_{\text{out}} = P_4 \sin\theta_4 \sin\phi_4$  (see Fig. 4). The processes we wish to consider are those with large  $m'$  and large  $p_{\text{out}}$ .

In order to understand the relationship of the double-scattering cross section to its bremsstrahlung background, let us discuss how these processes scale with  $m'$ ,  $p_{\text{out}}$ , and  $A$ . The dominant contribution to the bremsstrahlung matrix elements are of the form  $\alpha_s^3 s^2 t^{-3}$  (Ref. 10), so

$$\sigma_{\text{brem}}^6 \sim A s^{-2} \alpha_s^3 s^2 t^{-3}.$$

Ignoring structure functions and identifying  $\langle s \rangle \sim m'^2$  and  $\langle t \rangle \sim p_{\text{out}}^2$ , we have

$$\sigma_{\text{brem}}^6 \propto A \alpha_s^3 p_{\text{out}}^{-6}. \quad (4.1)$$

To see how the double-scattering part scales, notice that it can be written as the product of the differential cross section for the first collision and the differential probability for the second collision:

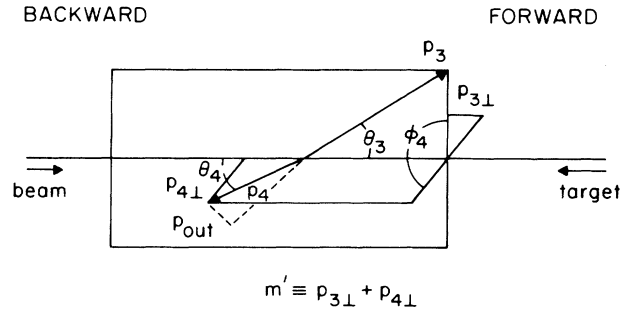


FIG. 4. Diagram defining  $p_{\text{out}}$  and  $m'$  in beam-nucleon c.m.s. The double-scattering model is applicable for large  $p_{\text{out}}$  and  $m'$ .

$$\sigma_{\text{double}}^6 \propto \frac{d\sigma}{dt_1} \frac{d(\text{prob})}{dt_2}. \quad (4.2)$$

The differential probability for the second collision scales as the product of the average path length to exit the nucleus,  $\langle l \rangle \sim A^{1/3} R_0$ , and the differential inverse mean free path,

$$\frac{d\lambda^{-1}}{dt_2} \propto \rho \frac{d\sigma}{dt_2}.$$

This results in

$$\frac{d\sigma}{dt_1} \propto \frac{A \alpha_s^2}{t_1^2}, \quad \frac{d(\text{prob})}{dt_2} \propto \frac{1}{R_0^3} A^{1/3} R_0 \frac{\alpha_s^2}{t_2^2}. \quad (4.3)$$

We see that double scattering scales as

$$\sigma_{\text{double}}^6 \propto \frac{A^{4/3} \alpha_s^4}{R_0^2} \frac{1}{p_{\text{out}}^8}. \quad (4.4)$$

Thus, bremsstrahlung and double scattering will give comparable contributions to nonplanar scattering for  $p_{\text{out}} \sim (A^{1/3} \alpha_s / R_0^2)^{1/2}$ . On tungsten ( $A = 184$ ), this is only  $p_{\text{out}} \sim 0.5$  GeV, a rather small number. For  $p_{\text{out}}$  much larger than this, the bremsstrahlung scattering gives the dominant contribution to these nonplanar events. Notice that for all values of  $p_{\text{out}}$ , double scattering increases the cross sections for these events.

To determine whether or not the double-scattering term gives a measurable effect at intermediate values of  $p_{\text{out}}$ , we must perform a more detailed calculation. The double scattering is enhanced relative to the bremsstrahlung scattering by a number of effects. First of all there is the factor of  $A^{1/3} \sim 2$  for Be ( $A = 9$ ) and  $\sim 6$  for W ( $A = 184$ ). A more important effect comes from the fact that the double-scattering events have three particles in the initial state. Because of this, the partons that generate the event can have smaller Feynman  $x$  than the bremsstrahlung partons and, as a result, double scattering can involve gluons from the region where the gluon structure function is large. The initial states containing one gluon from the target give a large contribution to double scattering. Also, since two separate collisions are involved, typical momentum transfers can be smaller, which further enhances their contribution to the cross section. The largest bremsstrahlung and double-scattering terms are plotted for  $A = 184$  (W) in Fig. 5

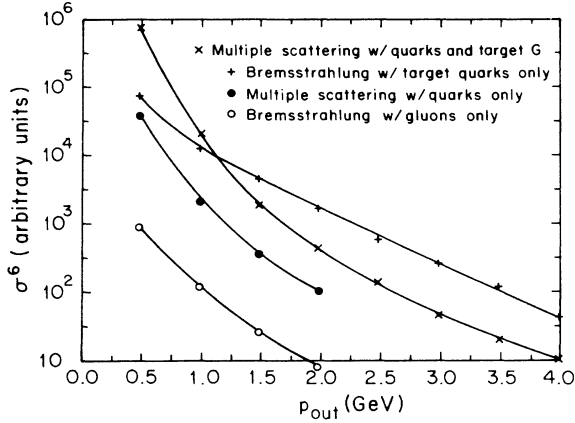


FIG. 5. Relative contributions of initial-state quarks and gluons to two-particle inclusive scattering,

$$\left\langle \frac{E_3 E_4 d\sigma^6}{dP_3^3 dP_4^3} \Big|_{p+A \rightarrow h^+ + h^- + X} \right\rangle.$$

Double-scattering and bremsstrahlung terms are plotted in arbitrary units for tungsten ( $A=184$ ) at  $E_{\text{lab}}=400$  GeV and  $m'=10.5$  GeV. Initial-state gluons from the target give an important contribution, but can be ignored elsewhere.

where curves with and without the gluon contributions are shown. Sea-quark contributions are small relative to the gluons and so are not considered here. Collisions with an initial-state gluon from the projectile also give negligibly small contributions to scattering. The projectile gluons can be ignored since the projectile parton must always be hard in order to create an event with a large transverse momentum, and the gluon structure functions are important only at small  $x$ . It is possible for one of the target partons to be fairly soft, however, since there will be another target parton to provide the remainder of the in-flowing energy. As can be seen from the plot, valence quarks dominate in the bremsstrahlung events, while events with one initial-state target gluon and events with all initial-state quarks give non-negligible contributions to double scattering.

Finally, to compare the model to data, expressions (2.9) and (2.10) are evaluated to obtain the double-differential cross section for producing unlike-sign hadrons using initial-state quarks in the bremsstrahlung term and quarks plus target gluons in the double-scattering term. We approximate the initial-state nucleons as isoscalars and proceed numerically using an adaptive Monte Carlo routine.<sup>11</sup> We take the  $qq \rightarrow qqG$  bremsstrahlung matrix elements from Ref. 10 and  $qq \rightarrow qq$  and  $qG \rightarrow qG$  matrix elements from Ref. 7. We use the structure functions of Ref. 12 and the fragmentation functions of Ref. 6. The result is plotted together with data in arbitrary units on Be, Cu, and W from Ref. 8 in Fig. 6. For each target, the upper curve gives the sum of bremsstrahlung and double scattering, while the lower curves are for bremsstrahlung scattering only. Here the data and curves are at  $E_{\text{lab}}=400$  GeV and  $m'=10.5$  GeV. In order to produce curves as a function of  $p_{\text{out}}$ , the cross section must be averaged over the region in phase space with the required  $m'$  and  $p_{\text{out}}$ .

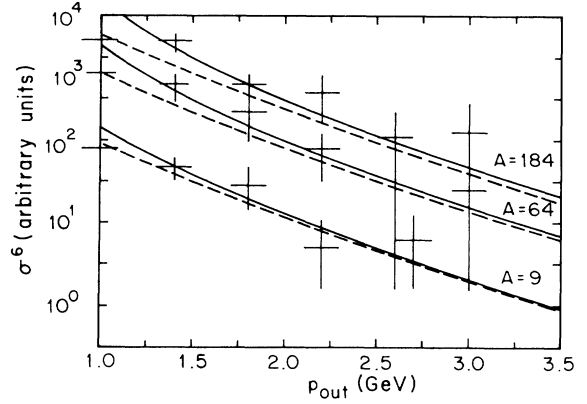


FIG. 6. Calculated two-particle inclusive cross sections,

$$\left\langle \frac{E_3 E_4 d\sigma^6}{dP_3^3 dP_4^3} \Big|_{p+A \rightarrow h^+ + h^- + X} \right\rangle,$$

on Be, Cu, and W for  $E_{\text{lab}}=400$  GeV and  $m'=10.5$  GeV are compared to data in arbitrary units from Ref. 8. The dashed curves are for bremsstrahlung scattering only while the solid curves represent both bremsstrahlung and double-scattering contributions.

The shape for the calculated curves is adequate for  $p_{\text{out}}$  down to roughly 1 GeV. Below 1 GeV, the double-scattering model becomes unreliable due to contributions from low- $x$  gluons ( $x \sim 0.01$ ). Predictions at 800 GeV laboratory energy are presented in Fig. 7. Evidently, more accurate measurements will be necessary to separate the multiple-scattering effect from the background for this process.

Multiple-scattering results are often expressed in terms of an exponent  $\alpha(p_{\text{out}})$  using the definition  $\sigma_{pA}^6 \equiv A^{\alpha(p_{\text{out}})} \sigma_{pN}^6$ . This eliminates the problem of overall normalization and is compared with data in Refs.

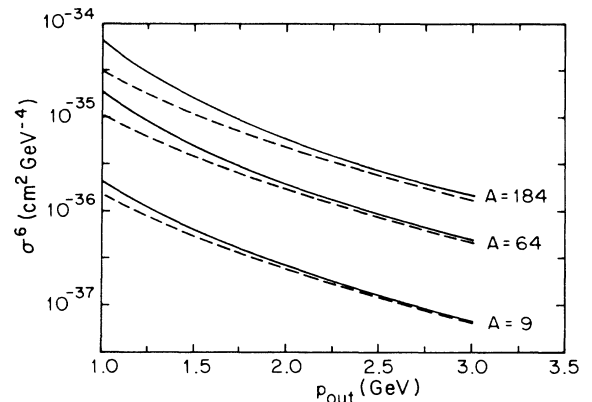


FIG. 7. Calculated two-particle inclusive cross sections,

$$\left\langle \frac{E_3 E_4 d\sigma^6}{dP_3^3 dP_4^3} \Big|_{p+A \rightarrow h^+ + h^- + X} \right\rangle (\text{cm}^2 \text{GeV}^{-4}),$$

on Be, Cu, and W for  $E_{\text{lab}}=800$  GeV and  $m'=10$  GeV. The dashed curves are for bremsstrahlung scattering only while the solid curves represent both bremsstrahlung and double-scattering contributions.

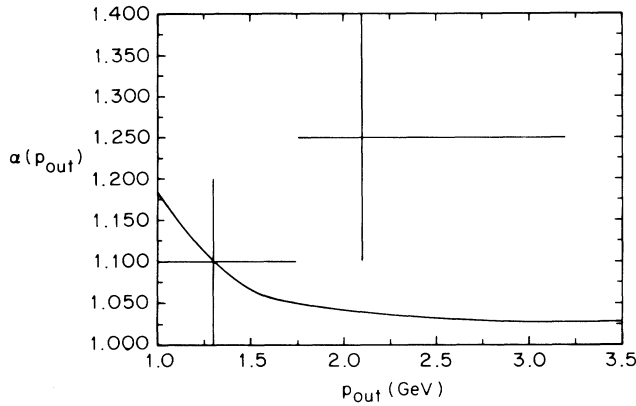


FIG. 8. Calculated  $\alpha(p_{\text{out}})$  for  $E_{\text{lab}}=400$  GeV and  $m'=10.5$  GeV compared to data (Refs. 8 and 9). This graph contains the same information as Fig. 6.

8 and 9 in Fig. 8. In the model,  $\alpha$  increases for small  $p_{\text{out}}$ , while in the data it decreases, becoming less than unity for  $p_{\text{out}} \sim 1$  GeV, as is the case for the analogous single-particle inclusive results.<sup>1</sup> Since all of the terms of (2.10) are positive, double scattering can only enhance the nonplanar cross section ( $\alpha > 1$ ). In order for  $\alpha(p_{\text{out}})$  to be less than unity in a multiple-scattering picture, shadowing must be important. This could involve a combination of absorption following bremsstrahlung  $O(\alpha_s^5)$ , triple scattering  $[O(\alpha_s^6)]$ , coherent, or nonperturbative effects. Another possibly important effect which has been ignored in the model is transverse-momentum smearing. However, transverse-momentum smearing most strongly effects the small- $x$  regions of the integrals, where we have seen that double scattering is much more sensitive than bremsstrahlung, so this should result in a relative enhancement of double scattering. In any event, transverse-momentum smearing cannot result in  $\alpha < 1$ . By way of conclusion, we see that although it is calculable, two-hadron nonplanar inclusive scattering may not be easy to study since it suffers from a large bremsstrahlung background.

## V. FORWARD-BACKWARD ASYMMETRY

In order to study double scattering by direct measurement of cross sections, we must disentangle it from the single-scattering background. Is there an alternative to just looking at the  $A$  dependence? In the proton-nucleon c.m.s., bremsstrahlung is symmetric with respect to the plane perpendicular to the beam (except for isospin). Thus, we expect the asymmetry measured by

$$\Delta \equiv \frac{\sigma^6(90^\circ > \theta_3, \theta_4 > 0^\circ) - \sigma^6(180^\circ > \theta_3, \theta_4 > 90^\circ)}{\sigma^6(90^\circ > \theta_3, \theta_4 > 0^\circ) + \sigma^6(180^\circ > \theta_3, \theta_4 > 90^\circ)} \quad (5.1)$$

to be nonzero only from multiple-scattering effects. Let  $F$  and  $B$  denote cross sections for both detected particles to lie in the forward (beam) and backward hemispheres, respectively. Assuming isoscalar scattering and using the decomposition of  $\sigma^6$  into bremsstrahlung and double-scattering components given by (2.9) and (2.10), the bremsstrahlung parts of the numerator cancel in the

forward and backward hemispheres. Writing the  $pN$  bremsstrahlung term as  $\sigma_{pN}^6$  and the  $pNN$  double-scattering term as  $\sigma_{pNN}^6$ , we can isolate the  $A$  dependence of the asymmetry. This gives

$$\Delta = \frac{A^{4/3}[\sigma_{pNN}^6(F) - \sigma_{pNN}^6(B)]}{A\sigma_{pN}^6(F+B) + A^{4/3}[\sigma_{pNN}^6(F) + \sigma_{pNN}^6(B)]} \quad (5.2)$$

A plot of  $\Delta$  vs  $p_{\text{out}}$  at  $E_{\text{lab}}=800$  GeV and  $m'=10$  GeV is given in Fig. 9. The phase-space-averaged background ( $FF+BB$ ) at  $p_{\text{out}}=1$  GeV is of order  $10^{-35}$  cm<sup>2</sup> GeV<sup>-4</sup> on tungsten and of order  $10^{-36}$  cm<sup>2</sup> GeV<sup>-4</sup> on beryllium.

Notice that  $\Delta$  changes sign at  $p_{\text{out}}=2.5$  GeV. This happens because scattering in which one of the target partons is at small  $x$  dominates for all but the largest values of  $p_{\text{out}}$ . The kinematics of producing two hadrons in the final state require that the projectile parton always have large Feynman  $x$  ( $\langle x_{\text{projectile}} \rangle \sim 0.5$  for  $p_{\text{out}} \sim 1$  GeV and  $m' \sim 10$  GeV at  $s=800$  GeV<sup>2</sup>). However, if one of the target partons is hard, the other can be quite soft (as small as  $x_{\text{target}} \sim 0.01$  while  $\langle x_{\text{target}} \rangle \sim 0.2$ ). This can be checked in the model by imposing a cut in the target  $x$  or by excluding gluons from the calculation. In either case,  $\sigma^6(B)$  becomes larger than  $\sigma^6(F)$  and  $\Delta$  changes sign. Experimentally, the same effect can be observed by imposing a cut in  $\phi_4$ . A cut at  $150^\circ$  reduces the signal by about an order of magnitude, but the signal/noise ratio still remains reasonable. Results for  $\Delta$  at  $E_{\text{lab}}=800$  GeV and  $m'=10$  GeV with a cut at  $\phi_4=150^\circ$  are given in Fig. 9.

The predictions for  $\Delta$  here are qualitative, in view of the lack of knowledge of gluon structure functions at these momentum transfers and small  $x$ . Also, the momenta of some of the participating partons and their momentum transfers can still be small in these nonplanar events ( $\sim 0.5$  GeV and  $\sim 0.5$  GeV<sup>2</sup>). The sensitivity of  $\Delta$  to  $F_{\text{glu}}$  can be seen in Table I. Here we present  $\Delta$  for structure functions of the form

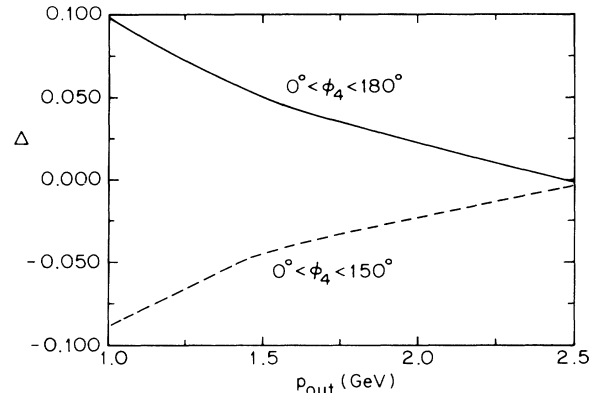


FIG. 9. Predictions for the forward-backward asymmetry  $\Delta$  of nonplanar two-particle inclusive scattering at  $E_{\text{lab}}=800$  GeV and  $m'=10$  GeV. Bremsstrahlung scattering makes no contribution to the signal in these events. The upper curve is for events from the entire kinematically allowed phase space where forward scattering dominates. For the lower curve,  $\phi_4$  is restricted to be less than  $150^\circ$  and backward-scattering events dominate.

TABLE I. Sensitivity of  $\Delta$  to the form of  $F_{\text{glu}}(x)$ . All results are for  $E_{\text{lab}} = 800$  GeV,  $m' = 10$  GeV, and  $p_{\text{out}} = 1$  GeV.

$F_{\text{glu}}(x)$	$\Delta_{\text{w}}$	$\Delta_{\text{Be}}$
0.57 $(1-x)^6 \frac{1}{x}$	0.10	0.06
0.513 $(1-x)^{12} \frac{1}{x}$	0.12	0.07
0.511 $(1-x)^{10} \frac{1}{x^{1.1}}$	0.15	0.1
0.511 $(1-x)^{10} \frac{1}{x^{0.9}}$	0.09	0.05

$$F_{\text{glu}}(x) = 0.5(k+1)x^{-1}(1-x)^k$$

and

$$F_{\text{glu}}(x) = 0.5 \times 11(1-x)^{10} x^{-(1+k)},$$

where  $k$  is a variable parameter. We see in the table that  $\Delta$  is not too sensitive to variations of the first form, but is moderately sensitive to variations of the second form.

Study of the forward-backward asymmetry of hadron nucleus collisions promises to be a new means of separating multiple-scattering events from single scattering. The asymmetry of two-particle inclusive events is explicitly calculable in multiple-scattering theory at  $O(\alpha_s^4 A^{4/3})$  and proves to be qualitatively sensitive to the gluon structure of the target.

## VI. SUMMARY

We have pointed out that incoherent QCD multiple-scattering production of single hadrons and planar pairs cannot be calculated in a cutoff-independent way using

Born cross sections. On the other hand, cross sections for nonplanar double-scattering events and their single-scattering bremsstrahlung background can be calculated without any cutoff. Double-scattering fits to data for nonplanar cross sections are adequate at large  $p_{\text{out}}$ . Double-scattering-induced forward-backward asymmetry in nonplanar scattering is calculated and found to be measurable, with the forward term dominating for most values of  $p_{\text{out}}$ . The forward-scattering dominance is caused by the small- $x$  structure of the target. If a cut in  $\phi_4$  is imposed, the small- $x$  effects are reduced and the sign of  $\Delta$  is reversed while its magnitude remains appreciable. With the cut in  $\phi_4$ , backward-scattering dominance is recovered, as expected from simple momentum conservation.

## ACKNOWLEDGMENTS

The author wishes to thank George Sterman for help and encouragement with this problem. Discussions with Robert McCarthy and David Jaffe proved very helpful in understanding its experimental status. This work was supported in part by the National Science Foundation under Grant No. Phy-85-07627.

## APPENDIX A: DERIVATION OF BREMSSTRAHLUNG CROSS SECTION

In this section we derive the two-particle inclusive cross section for the reaction  $H_1 + H_2 \rightarrow H_3 + H_4 + X$  producing hadrons  $H_3$  and  $H_4$  at high  $P_1$  in the c.m. for  $H_1$  and  $H_2$ . This is an extension of the usual result for  $H_1 + H_2 \rightarrow H_3 + X$  (Ref. 7):

$$E_3 \frac{d^3\sigma^{12 \rightarrow 3}}{dP_3^3} = \frac{1}{\pi} \sum_{ijk} \int dx_1 dx_2 F_1^i(x_1) F_2^j(x_2) \frac{1}{z_3} D_3^k(z_3) \frac{d\sigma^{ij \rightarrow k}}{d\hat{t}}(\hat{s}, \hat{t}, \hat{u}). \quad (\text{A1})$$

The momenta of the hadrons are  $P_1, P_2, P_3$ , and  $P_4$ , while the momenta of the partons are  $p_1, p_2, p_3$ , and  $p_4$ . The longitudinal-momentum fractions of the partons are  $x_1 = p_1/P_1$ ,  $x_2 = p_2/P_2$ ,  $z_3 = P_3/P_3$ , and  $z_4 = P_4/p_4$ . The six Mandelstam invariants describing the parton subprocesses can be expressed in terms of the hadron invariants and momentum fractions as

$$\begin{aligned} \hat{s} &= 2p_1 \cdot p_2 = 2x_1 x_2 P_1 \cdot P_2 = x_1 x_2 S, & \hat{s}' &= p_3 \cdot p_4 = 2 \frac{1}{z_3 z_4} P_3 \cdot P_4 = \frac{1}{z_3 z_4} S', \\ \hat{t} &= -2p_1 \cdot p_3 = -2x_1 \frac{1}{z_3} P_1 \cdot P_3 = x_1 \frac{1}{z_3} T, & \hat{t}' &= -2p_2 \cdot p_4 = -2x_2 \frac{1}{z_4} P_2 \cdot P_4 = x_2 \frac{1}{z_4} T', \\ \hat{u} &= -2p_1 \cdot p_4 = -2x_1 \frac{1}{z_4} P_1 \cdot P_4 = x_1 \frac{1}{z_4} U, & \hat{u}' &= -2p_2 \cdot p_3 = -2x_2 \frac{1}{z_3} P_2 \cdot P_3 = x_2 \frac{1}{z_3} U'. \end{aligned} \quad (\text{A2})$$

The partons scatter elastically so  $\hat{s} + \hat{t} + \hat{u} + \hat{s}' + \hat{t}' + \hat{u}' = 0$ .

The contribution of a given subprocess at fixed momentum fraction (the analog of  $d\sigma^{ij \rightarrow k}/d\hat{t} dx_1 dx_2 dz_3$  in the  $2 \rightarrow 2$  case) is

$$\frac{d\sigma^{ij \rightarrow kl}}{d\hat{t} d\hat{u} d\hat{t}' d\hat{u}' d\hat{s}' dx_1 dx_2 dz_3 dz_4} = \frac{d\sigma^{ij \rightarrow kl}}{d\hat{t} d\hat{u} d\hat{t}' d\hat{u}'} F^i(x_1) F^j(x_2) D^k(z_3) D^l(z_4) \delta(\hat{s} + \hat{t} + \hat{u} + \hat{s}' + \hat{t}' + \hat{u}'), \quad (\text{A3})$$

where  $d\sigma^{ij \rightarrow kl}/d\hat{t} d\hat{u} d\hat{t}' d\hat{u}'$  is the elastic  $2 \rightarrow 3$  cross section and the  $F$ 's and  $D$ 's are the parton structure and frag-

mentation functions, respectively. To get an expression in terms of the hadron momenta we use  $d\hat{t} = x_1(1/z_3)dt$ , etc., integrate over  $x_1, x_2, z_3$ , and  $z_4$ , and sum over parton flavors, with the result

$$\frac{d\sigma^{12 \rightarrow 34}}{d\hat{t} d\hat{u} d\hat{t}' d\hat{u}' d\hat{s}'} = \sum_{ijkl} \int dx_1 dx_2 dz_3 F_1^i(x_1) F_2^j(x_2) D_3^k(z_3) D_4^l(z_4) \frac{d\sigma^{ij \rightarrow kl}}{d\hat{t} d\hat{u} d\hat{t}' d\hat{u}'} \left[ \frac{x_1 x_2}{z_3 z_4} \right]^2 \times \frac{1}{z_3(\hat{s} + \hat{t} + \hat{u}')} \theta(z_4) \theta(1 - z_4), \quad (\text{A4})$$

where the  $z_4$  integral has been evaluated using

$$dz_4 \delta(\hat{s} + \hat{t} + \hat{u} + \hat{s}' + \hat{t}' + \hat{u}') = dz_4 \delta \left[ x_1 x_2 S + x_1 \frac{1}{z_3} T + x_1 \frac{1}{z_4} U + \frac{1}{z_3 z_4} S' + x_2 \frac{1}{z_4} T' + x_2 \frac{1}{z_3} U' \right] = dz_4 \frac{z_4}{\hat{s} + \hat{t} + \hat{u}'} \delta \left[ z_4 + \frac{x_1 U + \frac{1}{z_3} S' + x_2 T'}{\hat{s} + \hat{t} + \hat{u}'} \right] \theta(z_4) \theta(1 - z_4). \quad (\text{A5})$$

To get an expression in terms of c.m. angles and momenta, we use the  $2 \rightarrow 3$  phase space

$$S_{2 \rightarrow 3} = \int \frac{d^3 p_3}{(2\pi)^3 2\omega_3} \frac{d^3 p_4}{(2\pi)^3 2\omega_4} \frac{d^3 p_5}{(2\pi)^3 2\omega_5} (2\pi)^4 \delta^4(P - p_3 - p_4 - p_5) = \frac{1}{128\pi^4} \int \frac{d \cos(\theta_3) dp_3 d \cos(\theta_4) dp_4}{\sin(\theta_3) \sin(\theta_4) \sin(\phi_4)}. \quad (\text{A6})$$

With the Jacobian

$$\frac{\partial(\hat{t}, \hat{u}, \hat{t}', \hat{u}')}{\partial(p_3 \cos\theta_3 p_4 \cos\theta_4)} = 4\hat{s}^2 p_3 p_4,$$

the parton cross section is expressed in terms of the matrix element as

$$\frac{d\sigma^{ij \rightarrow kl}}{d\hat{t} d\hat{u} d\hat{t}' d\hat{u}'} = \frac{|M_{ij \rightarrow kl}(\hat{s}, \hat{t}, \hat{u}, \hat{s}', \hat{t}', \hat{u}')|^2}{1024\pi^4 \hat{s}^3 p_3 p_4 \sin\theta_3 \sin\theta_4 \sin\phi_4}. \quad (\text{A7})$$

Our final result for the cross section in terms of the hadron angles and momenta is obtained using the Jacobian

$$\frac{\partial(T, U, T', U', S')}{\partial(\phi_3 P_3 \cos\theta_3 P_4 \cos\theta_4)} = 8S^2 E_3^2 E_4^2 \sin\theta_3 \sin\theta_4 \sin\phi_4.$$

It is

$$E_3 E_4 \frac{d\sigma^{12 \rightarrow 34}}{dP_3^3 dP_4^3} = \frac{1}{256\pi^5 S^2} \sum_{ijkl} \int dx_1 dx_2 dz_3 \frac{F_1^i(x_1) F_2^j(x_2) D_3^k(z_3) D_4^l(z_4)}{(x_1 x_2 z_3)^2 z_4 \left[ 1 + \frac{\hat{t} + \hat{u}'}{\hat{s}} \right]} |M_{ij \rightarrow kl}|^2 \theta(z_4) \theta(1 - z_4), \quad (\text{A8})$$

where inside the integral  $z_4 = -(x_1 U + 1/z_3 S' + x_2 T') / \hat{s} + \hat{t} + \hat{u}'$ .

<sup>1</sup>J. W. Cronin *et al.*, Phys. Rev. D **11**, 3105 (1975); L. Kluberg *et al.*, Phys. Rev. Lett. **38**, 670 (1977); D. Antreasyan *et al.*, Phys. Rev. D **19**, 764 (1979).

<sup>2</sup>R. L. McCarthy *et al.*, Phys. Rev. Lett. **40**, 213 (1978); H. Jostlein *et al.*, Phys. Rev. D **20**, 53 (1979).

<sup>3</sup>R. Baier, J. Cleymens, K. Kinoshita, and B. Petersson, Nucl. Phys. **B118**, 139 (1977); R. D. Field and R. P. Feynman, Phys. Rev. D **15**, 2590 (1977).

<sup>4</sup>J. H. Kuhn, Phys. Rev. D **13**, 2948 (1976); A. Krzywicki, J. Engels, B. Petersson, and U. Sukhatme, Phys. Lett. **85B**, 407 (1979).

<sup>5</sup>M. Lev and B. Petersson, Z. Phys. C **21**, 155 (1983).

<sup>6</sup>J. F. Owens, E. Reya, and M. Gluck, Phys. Rev. D **18**, 1501 (1978).

<sup>7</sup>M. Gluck, J. F. Owens, and E. Reya, Phys. Rev. D **17**, 2324 (1978); B. L. Combridge, J. Kripfganz, and J. Ranft, Phys. Lett. **70B**, 234 (1977).

<sup>8</sup>Y. B. Hsiung, Ph.D. thesis, Columbia University, 1986.

<sup>9</sup>Y. B. Hsiung *et al.*, Phys. Rev. Lett. **55**, 457 (1985).

<sup>10</sup>A. Berends, R. Kleiss, P. De Causmaecker, R. Gastmans, and T. T. Wu, Phys. Lett. **103B**, 124 (1981).

<sup>11</sup>G. P. Lepage, J. Comput. Phys. **27**, 192 (1978).

<sup>12</sup>A. J. Buras and K. J. F. Gaemers, Nucl. Phys. **B132**, 249 (1977).